Supporting Information for

Zn(II)-bis(cyclen) complexes and the imaging of apoptosis/necrosis

D.Oltmanns[†], S. Zitzmann-Kolbe[‡], A. Mueller[‡], U. Bauder-Wuest[†], M. Schaefer[†], M. Eder[†], U. Haberkorn[§], M. Eisenhut[†*]

[†]Department of Radiopharmaceutical Chemistry, German Cancer Research Center, Im Neuenheimer Feld 280, 69120 Heidelberg, Germany; [‡]Global Drug Discovery, Bayer Healthcare, Berlin, Germany; [§]Department of Nuclear Medicine, University Hospital Heidelberg, Im Neuenheimer Feld 400, 69120 Heidelberg, Germany

Corresponding author: Michael Eisenhut, Ph.D.; Department of Radiopharmaceutical Chemistry, German Cancer Research Center, Im Neuenheimer Feld 280, 69120 Heidelberg, Germany; m.eisenhut@dkfz.de; T +49-6221-422443.

Table of Content	Page

Flow cytometry

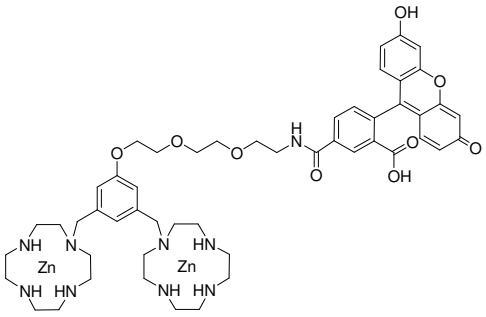

$[Zn_2 1]^{4+}$

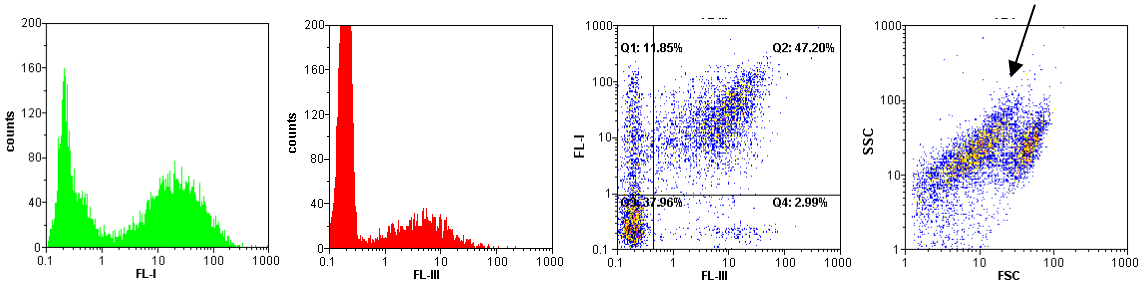

Staurosporine treated Jurkat cells, incubated with **$[Zn_2 1]^{4+}$** and PI.

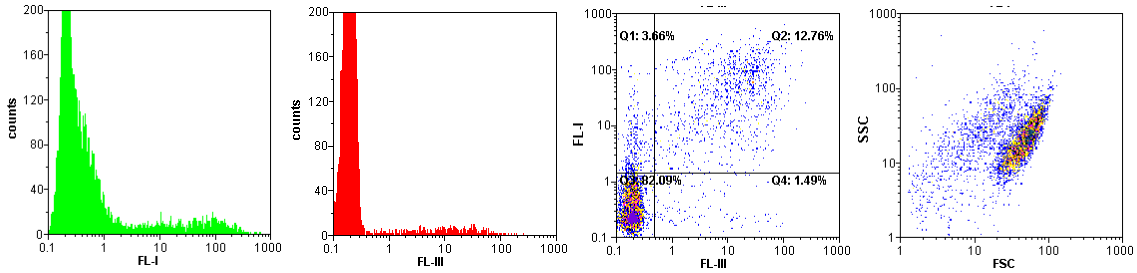

Non-treated Jurkat cells, incubated with **$[Zn_2 1]^{4+}$** and PI.

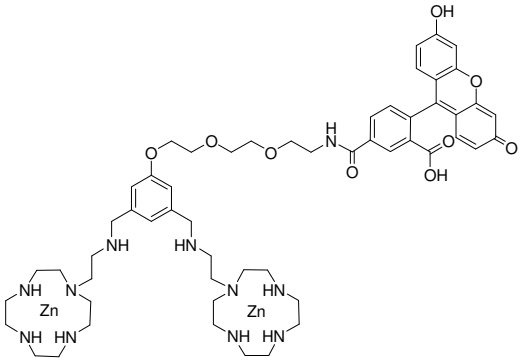

$[Zn_2 2]^{4+}$

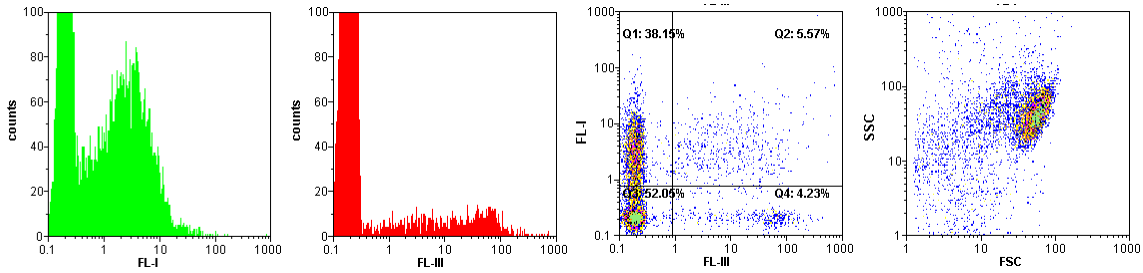

Staurosporine treated Jurkat cells, incubated with **$[Zn_2 2]^{4+}$** and PI.

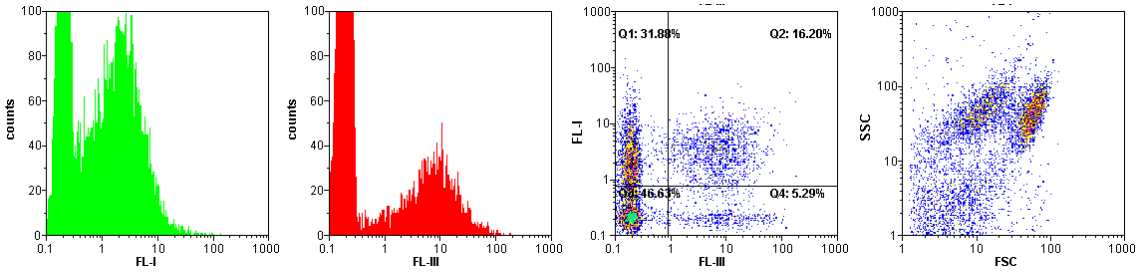

Non-treated Jurkat cells, incubated with **$[Zn_2 2]^{4+}$** and PI.

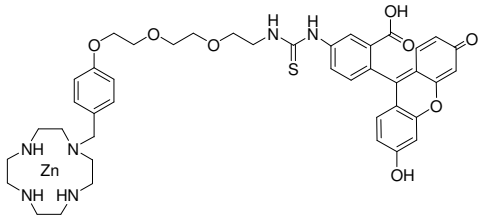

[Zn3]$^{2+}$

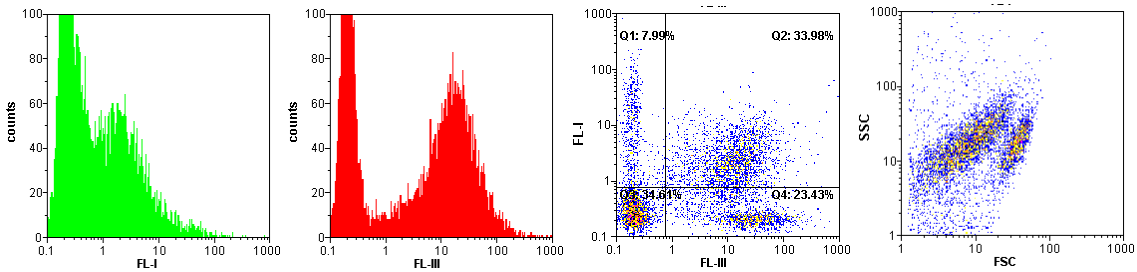

Staurosporine treated Jurkat cells, incubated with **[Zn3]$^{2+}$** and PI.

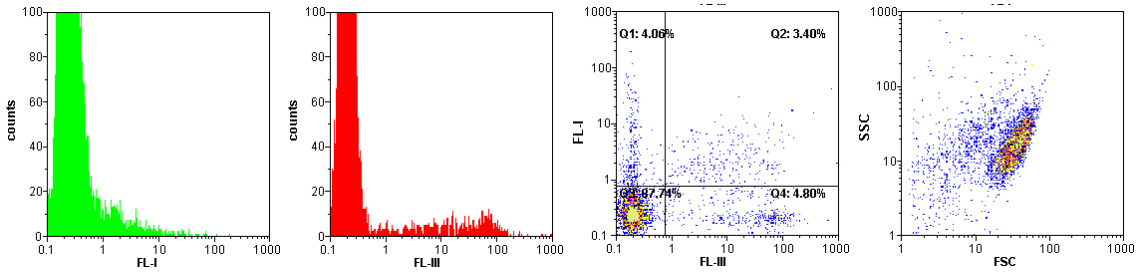

Non-treated Jurkat cells, incubated with **[Zn3]$^{2+}$** and PI.

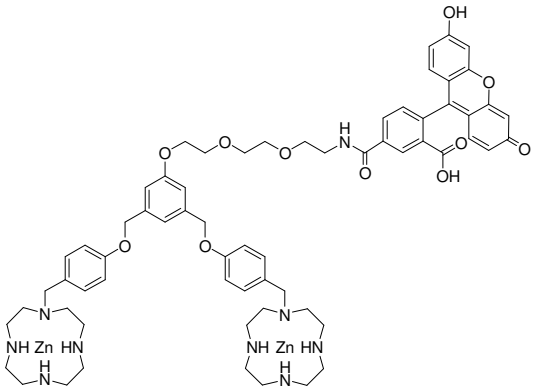

$[Zn_24]^{4+}$

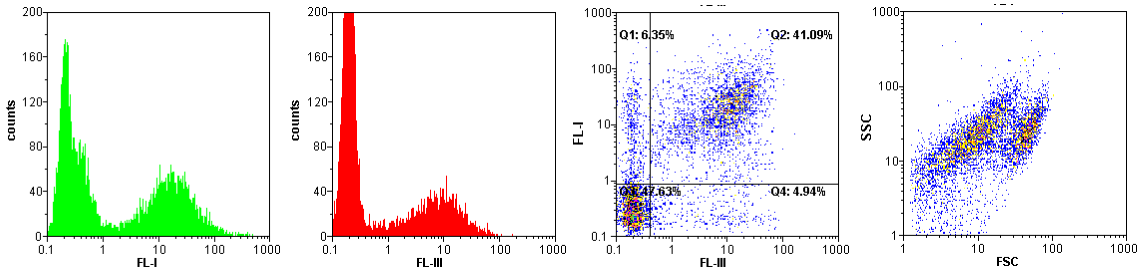

Staurosporine treated Jurkat cells, incubated with **$[Zn_24]^{4+}$** and PI.

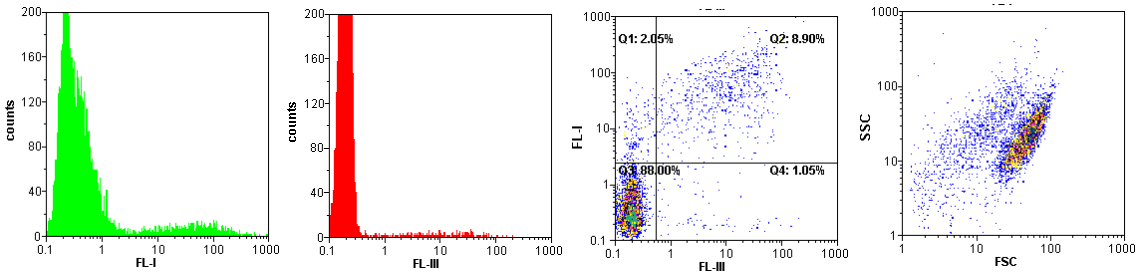

Non-treated Jurkat cells, incubated with **$[Zn_24]^{4+}$** and PI.

Complex ligand 4

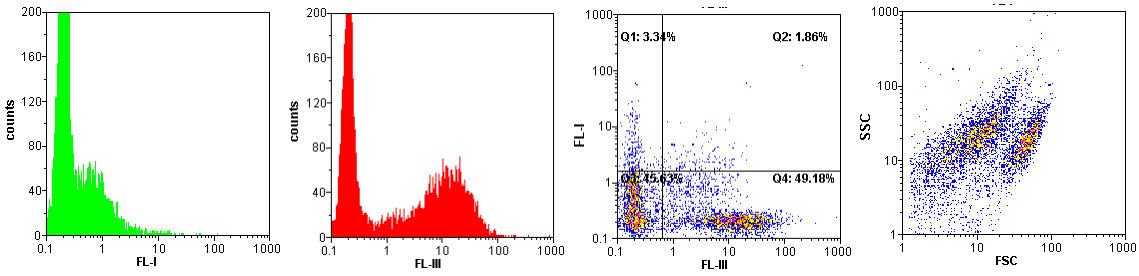

Staurosporine treated Jurkat cells, incubated with **4** and PI.

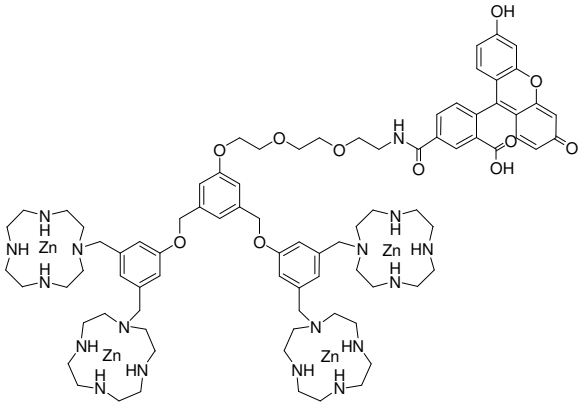

$[Zn_4 5]^{8+}$

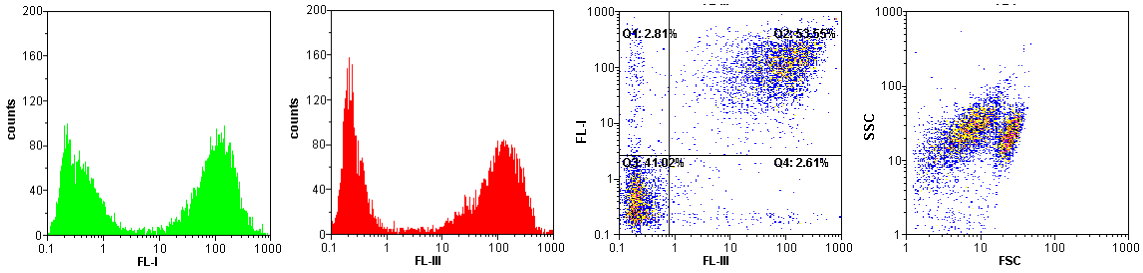

Staurosporine treated Jurkat cells, incubated with **$[Zn_4 5]^{8+}$** and PI.

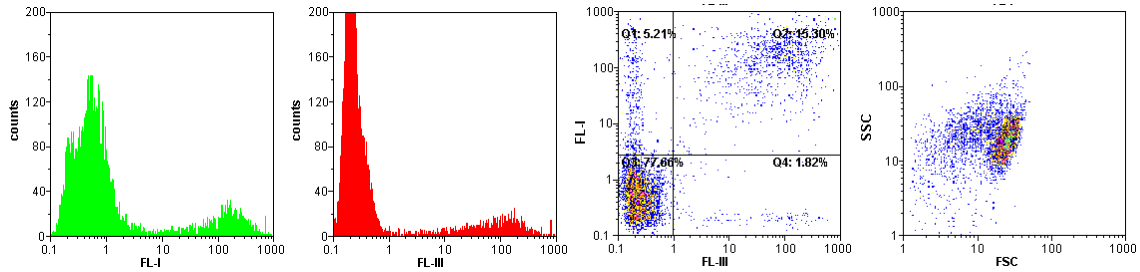

Non-treated Jurkat cells, incubated with **$[Zn_4 5]^{8+}$** and PI.

The role of CXCR4

Proof of CXCR4 expression

Staurosporine treated Jurkat cells

untreated Jurkat cells

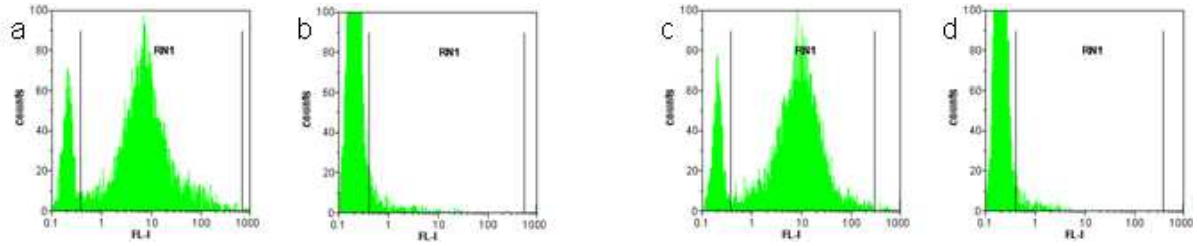

Flow cytometry of staurosporine induced (a,b) and untreated Jurkat cells (c,d). The cells were incubated with (a,c) the anti-CXCR4 mAb12G5 and the FITC labeled anti-mouse antibody and (b,d) with the FITC labeled anti-mouse antibody alone (control).

Competition experiment

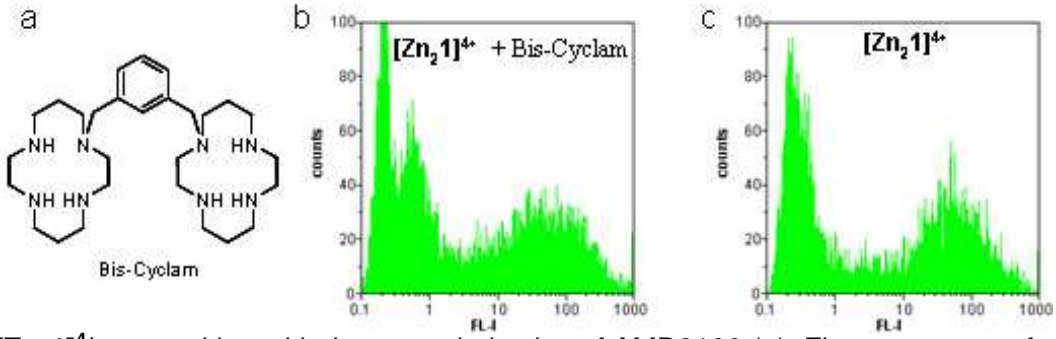

$[Zn_2 1]^{4+}$ competition with the meta derivative of AMD3100 (a). Flow cytometry of staurosporine treated Jurkat cells, incubated with **$[Zn_2 1]^{4+}$** in presence of a 100 fold molar excess of bis-cyclam b) and with **$[Zn_2 1]^{4+}$** alone (c).

Addendum to Figure 5

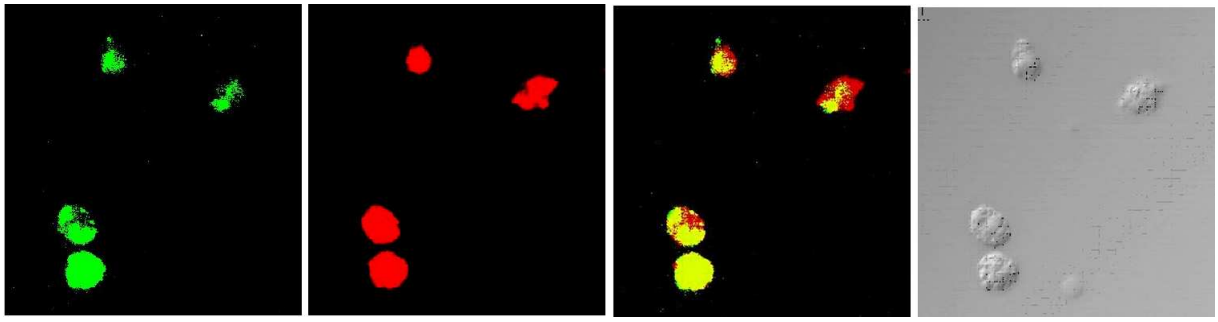

CLSM images of apoptosis induced Jurkat cells incubated with $\mathbf{[Zn_2 1]^{4+}}$ (green) and PI (red). Overlap of fluorescence images result in yellow colour. Phase contrast image on the right.

Cytotoxicity of $[Zn_2 1]^{4+}$

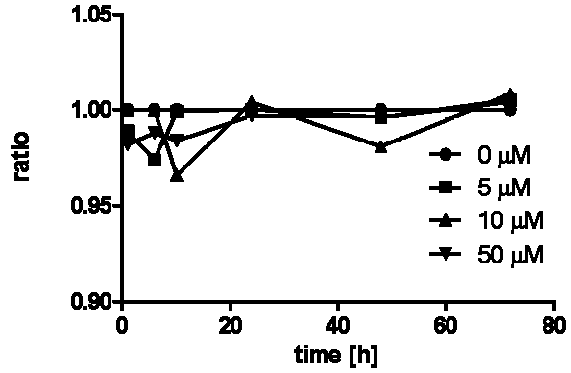

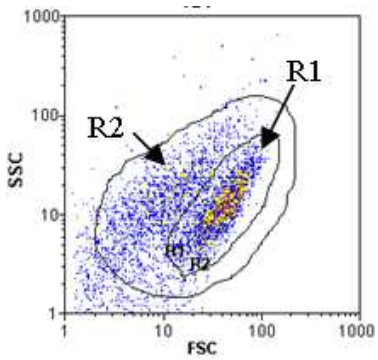

Vital Jurkat cells were incubated at 37°C in RPMI growth medium containing **$[Zn_2 1]^{4+}$** at concentrations of 0, 5, 10 and 50 µM for 1, 6, 10, 24, 48 and 72 hours. The integrity of the cells was analyzed using the flow cytometric sideward (SSC) and forward (FSC) scatter signals. According to the SSC/FSC-plot (example shown on the right) cells changing size and granularity (apoptotic and secondary necrotic cells; R2-R1) could be distinguished from vital/early apoptotic cells (R1). Up to concentrations of 50 µM the unchanged/altered cell fraction was only faintly depressed within the indicated time frame. The ratio is defined as R1/R2 with R1/R2 normalized to 1 at t=0 and 0 µM **$[Zn_2 1]^{4+}$**. Mean of three measurements; error bars were omitted because of clarity (all 50 µM values averaged to a ratio of 0.992±0.009). Lack of time dependent changes in the scatter plots of vital cells indicate negligible impact of the complex on the biology of Jurkat cells.

$[Zn_2(^{18}F\text{-}6)]^{4+}$ PET and addendum to Figure 6a

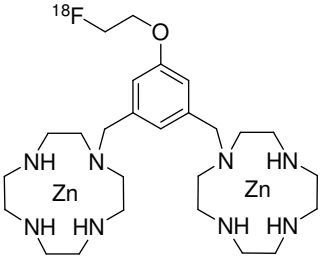

$[Zn_2\mathbf{1}]^{4+}$

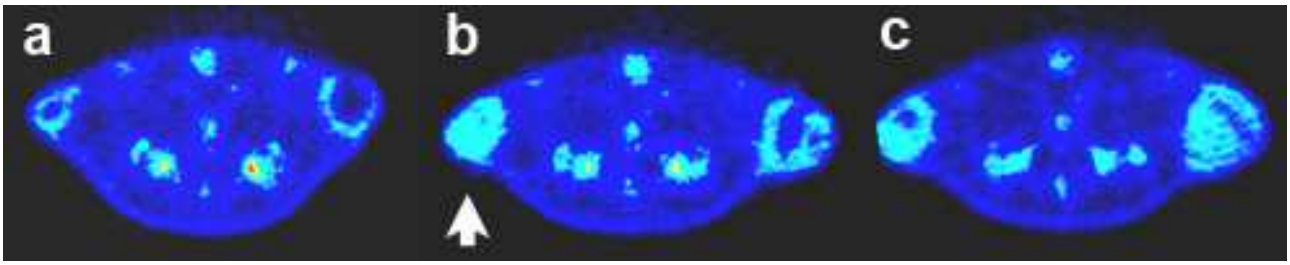

Transaxial $[Zn_2(^{18}F\text{-}6)]^{4+}$ PET images of a male Copenhagen rat with bilaterally transplanted Dunning R3327-AT1 prostate tumors. The 1 h PET images were obtained 1 day before (a), 6 (b) and 10 days (c) after irradiation with a single unilateral radiation dose of 50 Gy (arrow).

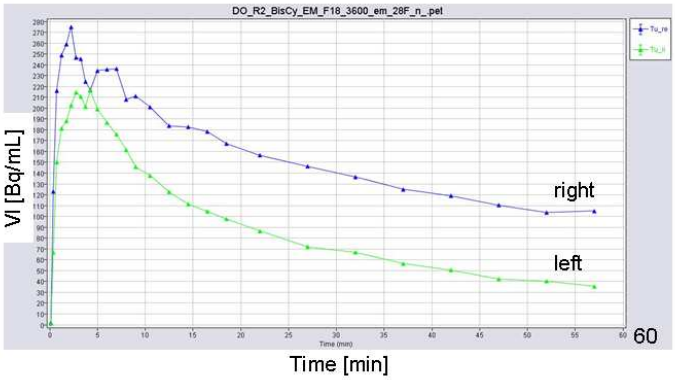

Time-activity curves of $[Zn_2(^{18}F\text{-}6)]^{4+}$ at day 6 after irradiation. ROI's were laid over the irradiated Dunning R3327-AT1 prostate tumor (blue) and control tumor (green).

$[Zn_2(^{18}F\text{-}6)]^{4+}$ PET and addendum to Figure 6b-d

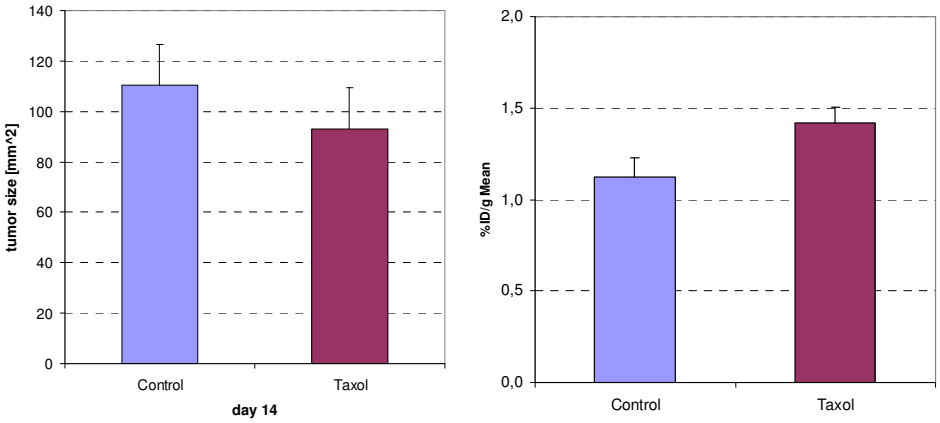

Mice with HelaMatu tumors were treated with 18 mg/kg Taxol at day 12 post inoculation. At day 14 tumor size was determined using a caliper. A trend towards decreased tumor size was found in taxol-treated tumors compare to controls. Tumor uptake of **$[Zn_2(^{18}F\text{-}6)]^{4+}$** (%ID/g) was determined by ROI analysis. The uptake of **$[Zn_2(^{18}F\text{-}6)]^{4+}$** was increased in the Taxol treated group as compared with uptake in the control animals (n=5 each).